

# CMS CALORIMETER TRIGGER IMPLEMENTATION AND PERFORMANCE

W. H. Smith, S. Dasu, M. Jaworski, J. Lackey  
*University of Wisconsin*

## 1. TRIGGER ALGORITHMS

The CMS level 1 trigger decision is based in part upon local information from the level 1 calorimeter trigger about the presence of physics objects such as photons, electrons, and jets, as well as global sums of  $E_t$  and missing  $E_t$  (to find neutrinos). Each of these physics is required to pass a series of  $p_t$  or  $E_t$  thresholds, which are used in making the Level 1 Trigger Decision.

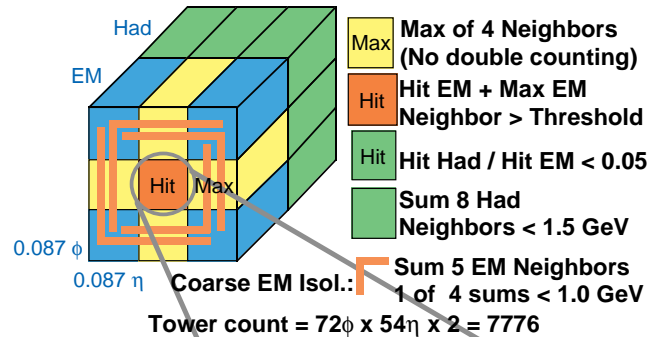
For most of the CMS ECAL, a 6 crystal by 6 crystal array of physical calorimeter towers is mapped into trigger towers. There is a 1:1 correspondence between the HCAL and ECAL trigger towers. The trigger tower size is equivalent to the HCAL physical towers,  $.087 \times .087$  in  $\eta \times \phi$ . The  $\phi$  size remains constant in  $\Delta\phi$  and the  $\eta$  size remains constant in  $\Delta\eta$  out to an  $\eta$  of 2.1, beyond which the  $\eta$  size doubles. There are 3888 total ECAL and 3888 total HCAL trigger towers from  $\eta = -2.6$  to  $\eta = 2.6$  ( $54 \times 72 \eta$ - $\phi$  divisions).

The electron/photon trigger is based on the recognition of a large and isolated energy deposit in the electromagnetic calorimeter by asking for a small hadronic energy deposit in the HCAL in the cluster region. There are different thresholds for inclusive electrons/photons, dileptons, and for very high  $E_t$  electrons. The isolation cuts are relaxed and finally eliminated for triggers with increasing  $E_t$  thresholds.

As shown in Figure 1, the basic 3x3 sliding window electron algorithm implemented in the hardware design involves two separate cuts on the longitudinal and transverse isolation of the ECAL energy deposit. The first cut involves the hit tower HCAL to ECAL energy ratio,  $H/E < 0.05$ . A second cut requires a cut on a sum of HCAL transverse energies in the nearest eight towers surrounding the hit tower,  $\Sigma_8 H < 2$  GeV. An optional ECAL transverse isolation of the electron/photon energy deposit is also possible by considering all four 5-tower corners of the 3x3 window and requiring that at least one of them is below a programmable cutoff  $\Sigma_5 E < 2$  GeV. The act of checking all four 5-tower corners ensures that the candidates depositing energy in any corner of the central tower do not self-veto due to leakage energy. Another optional cut that permits reduction of the electron energy threshold is based on a summary of the energy found in the ECAL crystals before summation in trigger towers. A “fine-grain” electromagnetic isolation bit is set and transmitted with the trigger tower energy if the maximum energy found in a pair of

strips of six crystals represents a large fraction of the total energy found in the 36 crystals summed.

### 3x3 Window Electron Trigger Algorithm:



### Fine-Grain Algorithm:

Use individual tower information from EM calorimeter to reduce electron/photon trigger rates:  
 Compare maximum of 5  $\eta$ -strip pair energy & total energy in trigger tower.

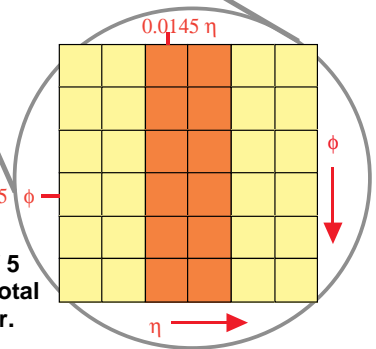


Figure 1. Level 1 Electron Trigger Algorithm.

The jet triggers are based on sums of ECAL and HCAL transverse energy in non-overlapping  $4 \times 4$  trigger tower ( $0.35 \eta \times 0.35 \phi$ ) regions. The jet trigger region sums have a 10-bit dynamic range covering energies up to about 1000 GeV. The jet trigger region sums are sorted based on their transverse energy to obtain top ranking jets. Tests of single, double, triple and quadruple jet region sums against progressively lower programmable thresholds, possibly in combination with electron and muon candidates, enables making level-1 trigger decision.

Neutrino identification consists of calculating the event missing  $E_t$  vector and testing it against a threshold. The calorimeter trigger calculates both sums of  $E_t$  and missing  $E_t$ . The transverse energy vector components are calculated from each 10-bit jet trigger region by multiplying with entries in corresponding lookup tables with angular coordinates. The sum of the scalar  $E_t$  and the vector components over the entire detector span made using digital summing networks provides

sum  $E_t$  and the missing  $E_t$ . When pre-scaled by factors of 1000 or more the unbiased sum  $E_t$  trigger enables checking other trigger efficiencies and measuring the  $E_t$  spectrum.

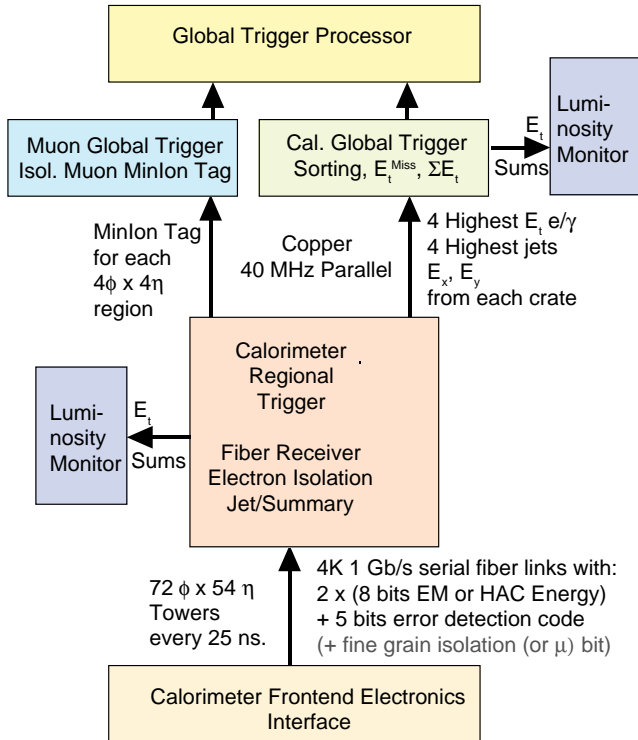


Figure 2. Overview of Level 1 Calorimeter Trigger.

## 2. CALORIMETER TRIGGER OVERVIEW

The calorimeter level 1 trigger system, shown in Figure 2, receives digital trigger sums via optical fibers from the front end electronics system, which transmits energy on an eight bit compressed scale. The data for two HCAL or ECAL trigger towers for the same crossing will be sent on a single fiber in eight bits apiece accompanied by five bits of error detection code and the ‘fine-grain’ bit described above.

The calorimeter regional crate system uses 19 calorimeter processor crates covering the full detector. Eighteen crates are dedicated to the barrel and two endcaps. These crates are filled out to an eta of 2.6, with partial utilization between 2.6 and 3.0. The remaining crate covers both Very Forward Calorimeters.

Each calorimeter regional crate transmits to the calorimeter global trigger processor its sum  $E_t$ ,  $E_x$  and  $E_y$ . It also sends its 4 highest-ranked electrons and 4 highest energy jets along with information about their location. The global calorimeter trigger then sums the energies and sorts the electrons and jets and forwards the top four calorimeter-wide electrons and jets, as well as the total calorimeter missing and sum  $E_t$  to the CMS global trigger.

The regional calorimeter trigger crate, shown schematically in Figure 3, has a height of 9U and a depth approximately of 700mm[1]. The front section of the crate is designed to accommodate 280mm deep cards, leaving the major portion of the volume for 400mm deep rear mounted cards.

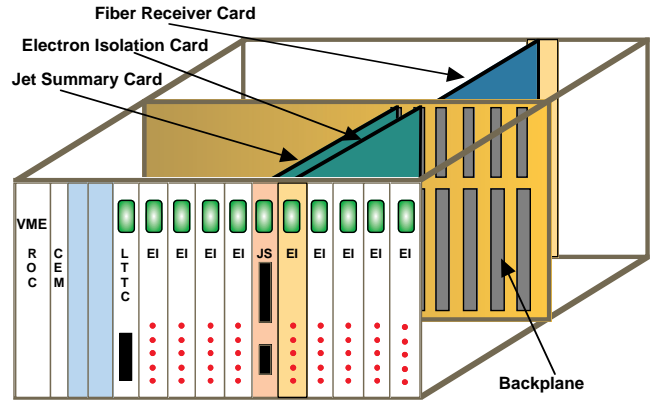


Figure 3. Schematic view of a typical Calorimeter Level 1 Regional crate.

The majority of cards in the Calorimeter Level 1 Regional Processor Crates, encompassing three custom board designs, are dedicated to receiving and processing data from the calorimeter. There are eight rear mounted Receiver cards, eight front mounted Electron Isolation cards, and one front mounted Jet Summary card for a total of 17 cards per crate.

The Receiver card is the largest board in the crate. It is 9U by 400mm. The rear side of the card receives the calorimeter data from optical fibers, translates from fibre to copper, and converts from serial to parallel format. The front side of the card contains circuitry to synchronize the incoming data with the local clock, and check for data transmission errors. There are also lookup tables and adder blocks on the front. The lookup tables translate the incoming information to transverse energy on several scales. The energy summation tree begins on these cards in order to reduce the amount of data forwarded on the backplane to the Jet Summary card. Separate cable connectors and buffering are also provided for intercrate sharing.

The transverse energy for each of the two 4 x 4 trigger tower regions is independently summed and forwarded to the Jet Summary card. On the Jet Summary card these  $E_t$  sums are used to continue the energy summation tree and also compared against a threshold to determine whether any sub-region contained jets. The  $E_t$  sums are applied to a set of lookup tables to generate  $E_x$  and  $E_y$  for each 4 x 4 region. A

[1] J. Lackey et al., CMS Calorimeter Level 1 Trigger Conceptual Design, CMS TN/94-284 (1994).

separate adder tree is used to sum up  $E_x$  and  $E_y$  from the regional values.

Though the input values at the top of the adder tree have only 8 bits of range, the adder tree has been designed to handle a dynamic range of 10 bits for either positive or negative values. This implies an overflow at approximately 1000 GeV, using the compressed scale described in the CMS Level 1 Calorimeter Trigger Performance Studies [2].

#### 4. ADDER ASIC

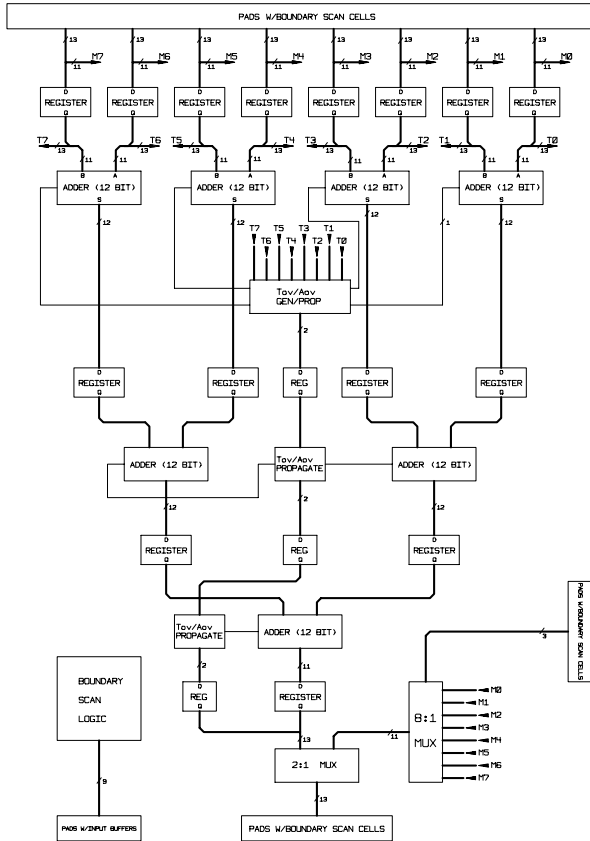


Figure 4. Block diagram of the Adder ASIC.

The adder ASIC is implemented as a 4-stage pipeline with eight input operands and 1 output operand. There are only three stages of adder tree, but an extra level of storage has been added to ensure chip processing is isolated from the I/O. We have determined that the ASIC must work reliably at a clock period of 5.0 nsec in order to ensure safe operation at an in-circuit period of 6.25 nsec. The adder tree is composed of 4 bit adder macro cells to implement twelve bit wide adders. Eleven bits are wired, left justified, to each operand of an adder. The LSB of each adder will be internally set to ZERO. The MSB is treated as a sign bit. Therefore, although the adder tree may

be constructed from three 4 bit adders, the width of the operand data paths has been limited to eleven bits.

The top of the adder tree is composed of four 12 bit adders and includes the logic required to detect and pass along overflows. Edge triggered registers are used to store the results for the next stage of the adder tree. A block diagram of the Adder ASIC is shown in Figure 4. The second stage contains two more 12 bit adders and includes the logic needed to propagate and detect overflows. Edge triggered registers are used to store the results for the next stage of the adder tree. The third stage contains the final adder as well as a continuation of the overflow circuitry. The register at this level is the last storage element before the ASIC output. We retain the identity of the tower overflow bits through the entire tree.

The ASIC has been produced by Vitesse in 0.6  $\mu$  H-GaAs, consists of approximately 11,000 cells, uses 4 W, has been simulated to function at 308 MHz and tested to 200 MHz, considerably above the 160 MHz requirement.

#### 5. CRATE BACKPLANE

The crate backplane is completely custom with a full 9U height. The top 3U is reserved for a 32 bit VME interface. The remaining 6U is used for the high speed data paths between individual cards. All signals in the trigger data portion of the backplane will be transmitted on point to point links at 160 MHz. This data rate was chosen because it offers the opportunity to compress the number of data lines on the backplane and in the pipelined data logic by a factor of four.

The backplane is a monolithic printed circuit board with front and back card connectors. The top 3U of the backplane holds 4 row (128 pin) DIN connectors, capable of full 32 bit VME. The first two slots of the backplane will, however, use three row (96 pin) DIN connectors in the P1 and P2 positions with the standard VME pinout. Thus, a standard VME module can be inserted in the first two stations. The form factor conversion to the remaining slots is performed on the custom backplane. The bottom 6U of the backplane, in the data processing section of the crate, utilizes a single high speed controlled-impedance connector for both front and rear insertion. The design is based around a 340 pin connector, by AMP Inc., to handle the high volume of data transmitted from the Receiver cards to the Electron Isolation and Jet Summary Cards.

The front and rear insertion of cards in the data processing section of the crate was chosen to allow greater separation between cards and to provide a more protected environment for the fibers connected to the rear mounted Receiver cards. The increased separation will promote better cooling of the cards, and will enable a wider selection of front panel components. The staggering of the slots between front and rear cards is shown in figure 5.

[2] S. Dasu et al. CMS Level 1 Calorimeter Trigger Performance Studies, CMS TN/94-285 (1994)

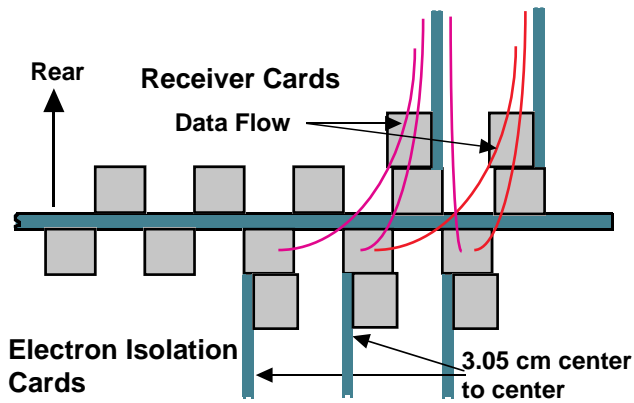


FIGURE 5. Design of crate backplane.

## 6. PERFORMANCE OF TRIGGER ALGORITHMS

We used a fast simulation program[3] to evaluate the performance of the calorimeter trigger algorithms. This program used the Pythia Monte Carlo to simulate several hundred thousand QCD jet and other physics events of interest. The response of the CMS detector was simulated for these events using a simplified geometry with a parameterized detector response. We simulated the sliding window algorithm, including the details of bit resolution and dynamic range as designed in the hardware, and obtained the electron/photon trigger QCD background rate and efficiency for detecting single electrons with minimum bias background. Hadronic isolation provides most of the rate reduction with high efficiency.

The jet trigger is important in the study of SUSY and QCD physics at the LHC. It supplements the missing  $E_T$  trigger for the study of squark and gluino production. When combined with the electron trigger it also provides a good  $\tau$  trigger. We performed a study of one, two, three and four-jet trigger rates and efficiencies for different summation regions. We examined transverse energy sums in single trigger towers,  $4 \times 4$  trigger tower regions and overlapping regions of  $8 \times 8$  trigger towers. We found that the non-overlapping  $4 \times 4$  trigger tower algorithm yields good performance. The performance is better for multijet triggers than that of the overlapping  $8 \times 8$  trigger tower algorithm[3]. The performance of the single tower trigger is poor. This preference for the  $4 \times 4$  algorithm had the additional benefit for the hardware that the missing  $E_T$  single hadron and total  $E_T$  triggers will all make use of the same  $0.35 \phi \times 0.35 \eta$  transverse energies[4].

The uncertainties in estimates of cross sections at high energies and limited knowledge of branching ratios impose a large error on the estimated trigger rates. In addition we cannot

assume that the CMS DAQ system will always run at its maximum design capacity. Therefore, we provide for a safety margin of a factor of three from the design 100 kHz maximum level 1 output rate to 30 kHz, in designing algorithms for level 1 triggers. Furthermore, this 30 kHz bandwidth of level 1 output has to be shared amongst both muon and calorimeter triggers. Therefore, we have selected a target rate of 15 kHz for the total output of all calorimeter triggers.

The individual calorimeter level 1 triggers are combined into a set of triggers used to provide the final trigger decision. These triggers include single and double photon/electron, single, 2, 3, and 4 jet triggers, a single electron combined with a single jet, a missing transverse energy trigger and a total transverse energy trigger. As discussed above, the target rate for this combination of calorimeter level 1 triggers is 15 kHz at the LHC design luminosity of  $10^{34} \text{cm}^{-2} \text{s}^{-1}$ .

We have selected a nominal set of energy cutoffs for these calorimeter triggers that yields, on balance, good efficiency for the various physics signals sought by CMS. The  $p_T$  cutoffs chosen are 400 GeV for total transverse energy, 80 GeV for missing transverse energy, 25 GeV for single electrons, 12 GeV for dielectrons, 100 GeV for a single jet, 60 GeV for dijets, 30 GeV for 3 jets, and 20 GeV for 4 jets. Finally there is a combination trigger requiring a jet above 50 GeV and an electron above 12 GeV.

Trigger Type	Trigger Et Cutoff (GeV)	Indiv. Rate (kHz)	Cumul. Rate (kHz)	Increm. Rate (kHz)
Sum Et	400	0.48	0.48	0.48
Miss Et	80	1.29	1.7	1.22
Single e	25	6.84	8.34	6.64
Double e	12	1.45	9.52	1.18
Single jet	100	2.06	10.7	1.16
Double jet	60	2.17	11.6	0.93
Triple jet	30	3.16	13.3	1.7
Quad jet	20	2.96	14.3	0.59
Jet + e	50 & 12	1.35	14.9	0.59

TABLE 1. Individual, cumulative, and incremental level 1 calorimeter trigger rates for QCD jet events at a luminosity of  $10^{34} \text{cm}^{-2} \text{s}^{-1}$ .

Table 1 shows the rates for QCD jet events from these individual triggers at the luminosity of  $10^{34} \text{cm}^{-2} \text{s}^{-1}$ . This table also presents the cumulative rate and the contribution from the triggers as each is added in the order shown. The largest contribution to the rate, approximately 6.6 kHz of the 15 kHz total, is the single electron trigger. As the presence of an electron is required in a majority of the physics signals involving the calorimeter, it is important to allocate a significant portion of the allowed bandwidth to this trigger. All of the other triggers add about 1 kHz each to the total rate.

[3] S. Dasu et al., CMS Level 1 Calorimeter Trigger Performance on Technical Proposal Physics, CMS-TN-95-183, 1995.

[4] S. Dasu, et al., CMS Missing Energy Trigger Studies, CMS TN/95-111, 1995.

The variety of jet triggers is chosen to provide as unbiased a trigger with as low thresholds as possible to capture new physics such as SUSY.

CMS expects that certain higher cross section processes can be studied by exploiting lower thresholds that can be used at lower luminosity,  $L = 10^{33} \text{cm}^{-2} \text{s}^{-1}$ . In order to study those processes we selected another set of representative level-1 trigger energy cutoffs. The cutoffs and corresponding individual and cumulative rates are shown in Table 2. The electron trigger is emphasized in order to provide high efficiency for lower background leptonic channels such as those due to top decays. The  $E_t$  trigger energy cutoffs have also been reduced substantially to increase efficiencies from less biased triggers.

Trigger Type	Trigger Et Cutoff (GeV)	Indiv. Rate (kHz)	Cumul.. Rate (kHz)	Increm. Rate (kHz)
Sum Et	150	1.04	1.04	1.04
Miss Et	40	2.11	2.82	1.78
Single e	12	10.3	12.3	9.5
Double e	7	1.54	13.1	0.76
Single jet	50	1.98	13.5	0.42
Double jet	30	1.63	13.9	0.42
Triple jet	20	1.02	14.1	0.18
Quad jet	15	0.68	14.2	0.08
Jet + e	15 & 9	5.98	15.2	1.02

TABLE 2. Individual, cumulative, and incremental level 1 calorimeter trigger rates for QCD jet events at a luminosity of  $10^{33} \text{cm}^{-2} \text{s}^{-1}$ .

We studied the acceptance of the calorimeter trigger for an 80 GeV standard model Higgs decaying to two photons and a 120 GeV Higgs decaying to  $ZZ^*$  producing an electron[3]. We chose the lighter Higgs masses because triggering on electrons becomes easier at higher Higgs masses. We also studied a 200 GeV Higgs decay to two real Z bosons followed by at least one Z decay to an  $e^+e^-$  pair. Since the Higgs production cross section is low even at the LHC, these studies were done at a luminosity of  $10^{34} \text{cm}^{-2} \text{s}^{-1}$ .

We found 97.4% efficiency for 80 GeV Higgs events that decay to two photons, 76.4% efficiency for 120 GeV Higgs events that decay to  $ZZ^*$ , with a subsequent Z or  $Z^*$  decay to  $e^+e^-$  and  $\mu^+\mu^-$  (which becomes almost 100% when muon triggers are added), and 99.1% for 200 GeV Higgs decays to ZZ followed by one of the Z decays to an  $e^+e^-$  pair and another to two jets, all within the detector fiducial volume. The above results also indicate good trigger performance for Higgs decays to  $l\nu\nu$  even for masses well below the 500 GeV considered in the CMS Technical Proposal.

We have examined the performance of the calorimeter trigger on the minimal supersymmetric Standard Model

(MSSM) with a charged Higgs state, two CP-even states ( $h^0$ ,  $H^0$ ), and one CP-odd ( $A^0$ ) neutral state. Since the cross section for the production of these SUSY Higgs is expected to be large for the parameter range selected, we studied the trigger performance at the low luminosity,  $L = 10^{33} \text{cm}^{-2} \text{s}^{-1}$ .

Tables 3 and 4 summarize our results on the performance of the CMS calorimeter trigger on physics processes described as important physics goals in the CMS technical proposal[5]. These processes include both standard and MSSM Higgs production, and SUSY squark and gluino searches. The evaluations have been made using the selected set of trigger cutoffs at the luminosities of  $10^{34} \text{cm}^{-2} \text{s}^{-1}$  and  $10^{33} \text{cm}^{-2} \text{s}^{-1}$  shown in Tables 1 and 2 respectively. The phrase, "SUSY CMS TP Scenario A" in Table 3 refers to the CMS Technical Proposal scenario A for SUSY, which is the scenario where triggering is the most difficult. These studies have been used in the determination of the CMS collaboration calorimeter trigger algorithms[6].

Process	Efficiency(%)
H (80 GeV) $\rightarrow \gamma\gamma$	97.4
H (120GeV) $\rightarrow ZZ \rightarrow ee\mu\mu$	76.4*
H (200 GeV) $\rightarrow ZZ \rightarrow eejj$	99.1
$pp \rightarrow tt \rightarrow eX$	88.3
$pp \rightarrow tt \rightarrow H + X \rightarrow tX$	81.7
SUSY CMS TP Scenario A ( $M_{LSP} = 45, M_{\text{split}} \sim 300$ GeV)	97.8
SUSY Neutral Higgs (Range of $\tan\beta$ and $M_H$ values)	45 - 98

TABLE 3. Physics process efficiency at  $L = 10^{34} \text{cm}^{-2} \text{s}^{-1}$ .

Process	Efficiency(%)
$pp \rightarrow tt \rightarrow eX$	99.3
$pp \rightarrow tt \rightarrow H + X \rightarrow tX$	99.0
$pp \rightarrow bb$ (hadronize), $B \rightarrow eX$	0.2 (but 400 Hz)
SUSY CMS TP Scenario A ( $M_{LSP} = 45, M_{\text{split}} \sim 300$ GeV)	97.8
SUSY Neutral Higgs (Range of $\tan\beta$ and $M_H$ values)	45 - 98

TABLE 4. Physics process efficiency at  $L = 10^{33} \text{cm}^{-2} \text{s}^{-1}$ .

This work is supported by the United States Department of Energy and the University of Wisconsin.

[5] CMS, The Compact Muon Solenoid Technical Proposal, CERN/LHCC 94-38, 15 December 1994.

[6] J. Varela et al., Preliminary specification of the baseline calorimeter trigger algorithms, CMS-TN/96-010, 1996.